environmental microbiology

Environmental Microbiology (2020) **22**(6), 2124–2139 doi:10.1111/1462-2920.14969

# Sulphide addition favours respiratory ammonification (DNRA) over complete denitrification and alters the active microbial community in salt marsh sediments

**Anna E. Murphy**,[1,2*] **Ashley N. Bulseco**,[1,3] **Ross Ackerman**,[4] **Joseph H. Vineis**[1] **and Jennifer L. Bowen**[1]

[1]*Department of Marine and Environmental Sciences, Marine Science Center, Northeastern University, Nahant, Massachusetts, 01908, USA.*

[2]*INSPIRE Environmental, Inc, 513 Broadway Suite 314, Newport, Rhode Island, 02840, USA.*

[3]*The Ecosystems Center, Marine Biological Laboratory, Woods Hole, Massachusetts, 02543, USA.*

[4]*Biology Department, Bates College, Lewiston, Maine, 04240, USA.*

## Summary

**The balance between nitrate respiration pathways, denitrification and dissimilatory nitrate ($NO_3^-$) reduction to ammonium (DNRA), determines whether bioavailable nitrogen is removed as $N_2$ gas or recycled as ammonium. Saltwater intrusion and organic matter enrichment may increase sulphate reduction leading to sulphide accumulation. We investigated the effects of sulphide on the partitioning of $NO_3^-$ between complete denitrification and DNRA and the microbial communities in salt marsh sediments. Complete denitrification significantly decreased with increasing sulphide, resulting in an increase in the contribution of DNRA to $NO_3^-$ respiration. Alternative fates of $NO_3^-$ became increasingly important at higher sulphide treatments, which could include $N_2O$ production and/or transport into intracellular vacuoles. Higher 16S transcript diversity was observed in the high sulphide treatment, with clear shifts in composition. Generally, low and no sulphide, coupled with high $NO_3^-$, favoured the activity of Campylobacterales, Oceanospirillales and Altermonadales, all of which include opportunistic denitrifiers. High $\sum$sulphide conditions promoted the activity of potential sulphide oxidizing nitrate reducers (Desulfobulbaceae, Acidiferrobacteraceae and Xanthomonadales) and sulphate reducers (Desulfomonadaceae, Desulfobacteraceae). Our study highlights the tight coupling between N and S cycling, and the implications of these dynamics on the fate of bioavailable N in coastal environments susceptible to intermittent saltwater inundation and organic matter enrichment.**

## Introduction

Coastal sediments are important sites for biogeochemical cycling including carbon (C) and nitrogen (N) cycles. Sharp gradients of oxygen, organic C, N and sulphur species result in tight coupling among microbial processes that transform and cycle these elements. In these sediments, denitrification, the microbial transformation of nitrate ($NO_3^-$) to inert nitrogen gas ($N_2$), occurs under anoxic conditions when $NO_3^-$ is available. Denitrification serves as an important sink for bioavailable N, particularly in coastal systems plagued by excess nutrient inputs, which, without removal, can result in eutrophic conditions (Nixon, 1995). Microorganisms that conduct dissimilatory nitrate reduction to ammonium (DNRA), also referred to as respiratory ammonification, an understudied, yet important microbial metabolism in coastal sediments, competes with denitrifiers for substrates, both $NO_3^-$ and organic carbon (Giblin *et al*., 2013). DNRA, however, recycles bioavailable N in the environment while denitrification removes it, so the partitioning of $NO_3^-$ across these two pathways is of great ecological importance. An understanding of what controls rates of denitrification and DNRA in coastal sediments is critical to understand shifts in these biogeochemical functions in response to stressors.

Both DNRA and denitrification are typically organotrophic metabolisms, in which microorganisms reduce $NO_3^-$ while oxidizing organic carbon (Tiedje, 1988). These pathways exist across a phylogenetically expansive range of microorganisms and, although originally thought to be mutually exclusive, the co-occurrence of the genes mediating both pathways in single genomes have been observed (Sanford *et al*., 2012; Mania *et al*., 2014; Yoon *et al*., 2015). Several

Received 5 October, 2019; revised 14 February, 2020; accepted 28 February, 2020. *For correspondence. E-mail an.murphy@northeastern.edu; Tel. (781)718-2836.

© 2020 Society for Applied Microbiology and John Wiley & Sons Ltd.

studies report that the availability of labile organic C relative to $NO_3^-$ correlates with the relationship between denitrification and DNRA, with DNRA becoming more important when the ratio of labile organic C to $NO_3^-$ is high (Algar and Vallino, 2014; Kraft *et al*., 2014; Hardison *et al*., 2015; Yoon *et al*., 2015). However, both DNRA and denitrification can also occur through chemolithotrophic metabolism, in which a reduced inorganic species, such as reduced sulphur, is oxidized through $NO_3^-$ reduction (e.g. Sayama *et al*., 2005; Cardoso *et al*., 2006; Tikhonova *et al*., 2006).

High concentrations of sulphide and hydrogen sulphide (i.e. $H_2S$, $HS^-$ and $S^{2-}$), hereafter ∑sulphide, may significantly affect the partitioning of $NO_3^-$ between denitrification and DNRA through several mechanisms. ∑Sulphide inhibits nitrification (Joye and Hollibaugh, 1995), the two-step aerobic chemolithotrophic process that oxidizes ammonium ($NH_4^+$) to nitrite ($NO_2^-$) and then to $NO_3^-$. By doing so, ∑sulphide may indirectly promote DNRA over denitrification by increasing the ratio of labile C to $NO_3^-$. ∑Sulphide may also directly inhibit the last step in denitrification, where nitrous oxide ($N_2O$) is transformed to $N_2$ (Sorensen *et al*., 1980; Brunet and Garcia-Gil, 1996; Senga *et al*., 2006). However, ∑sulphide may promote denitrification and/or DNRA by serving as an electron donor for these $NO_3^-$ reduction pathways. For example, ∑sulphide-dependent denitrification is reported in numerous settings including the Baltic Sea (Hannig *et al*., 2007; Hietanen *et al*., 2012; Dalsgaard *et al*., 2013) and the Mariager Fjord (Jensen *et al*., 2009). In the Baltic Sea, ∑sulphide concentrations up to 40 μM stimulated denitrification rates while DNRA rates were either unaffected or increased above this ∑sulphide concentration (Bonaglia *et al*., 2016). Thus, although it may serve as an electron donor for either denitrification or DNRA, ∑sulphide can also inhibit these pathways by limiting the substrate and creating toxic conditions. Furthermore, there have been no studies that directly investigate the shifts in microbial community structure that results from ∑sulphide additions and that plays a key role in the partitioning of $NO_3^-$ respiration between denitrification and DNRA in sediments.

∑Sulphide, products of sulphate ($SO_4^{2-}$) reduction, is high in organic-rich coastal sediments with high anaerobic respiration rates, such as salt marsh sediments (e.g. Bradley and Dunn, 1989; Rey *et al*., 1992). ∑Sulphide may also accumulate in tidal freshwater sediments exposed to salt-water intrusion as a result of storm surges and sea-level rise that delivers $SO_4^{2-}$-rich seawater upstream, and promotes $SO_4^{2-}$ reduction (Weston *et al*., 2006). Tidal wetland sediments are characterized by complex redox gradients, with very shallow oxygen penetration, concurrent with steep horizontal redox gradients from oxygen production in the rhizosphere. The close spatial proximity of ∑sulphide, $NO_3^-$ and labile organic C, fuels taxonomically and metabolically diverse microbial communities, with the capacity to rapidly respond to changes in substrate availability and redox conditions (Graves *et al*., 2016; Bulseco *et al*., 2019). Within this context, our study aimed to determine the effect of ∑sulphide concentration on the partitioning of $NO_3^-$ between DNRA and denitrification and to investigate the microbial community shifts responsible for these metabolic shifts. Specifically, we hypothesized that under high $NO_3^-$ concentrations and anoxic conditions, elevated ∑sulphide concentrations would decrease $N_2$ production and increase $NH_4^+$ production through DNRA. We expected elevated ∑sulphide concentrations to have a significant effect on the active microbial community and specifically promote the activity of taxa capable of oxidizing reduced sulphur.

## Results

### *Biogeochemical measurements*

The effects of ∑sulphide concentrations (0, 10, 100 and 1000 μM) on the rates of microbially mediated N transformations were tested using anoxic salt marsh sediment slurry, time series, batch incubations spiked with isotopically labelled $^{15}NO_3^-$ and tracing this isotope into the various N pools. Within each ∑sulphide treatment, total $NH_4^+$ (i.e. $^{14+15}NH_4^+$), $^{15}NH_4^+$ and $^{29+30}N_2$, all significantly increased over time, while concentrations of $NO_x^-$ significantly decreased during the incubation (Table 1; Fig. 1). Within the 0 and 10 μM ∑sulphide treatments, $^{29+30}N_2$ production significantly exceeded $^{15}NH_4^+$ production, as indicated by a significant interaction between analyte and time (ANCOVA interaction term; 0 μM: $F_{1,17} = 40.31$, $p < 0.001$; 10 μM: $F_{1,20} = 7.49$, $p = 0.01$, Fig. 1). While for the 100 μM ∑sulphide treatment, there was no significant difference in production rates of $^{29+30}N_2$ and $^{15}NH_4^+$ as indicated by similar slopes (ANCOVA interaction term $F_{1,18} = 0.07$, $p = 0.80$, Fig. 1). $^{15}NH_4^+$ production was significantly higher than $^{29+30}N_2$ production in the 1000 μM ∑sulphide treatment (ANCOVA interaction term, $F_{1,17} = 5.32$, $p = 0.03$, Fig. 1).

Average rates of N cycle processes were calculated as the change in product or substrate concentration over time and are provided for each ∑sulphide treatment in Table 2. Consumption of $NO_x^-$ was not significantly different across ∑sulphide treatments, averaging −41.1 (±2.3) nmol $g^{-1}$ WW $h^{-1}$. Total $NH_4^+$ production was significantly higher in the 100-μM treatment compared with the 0 μM but was similar between 10, 100 and 1000 μM. Complete denitrification significantly decreased as ∑sulphide concentrations increased, with rates that ranged from 10.0 (±0.4) nmol g $WW^{-1}$ $h^{-1}$ in the 1000 μM treatment to 26.3 (±0.6) nmol $g^{-1}$ WW $h^{-1}$ in the 0 μM treatment. For DNRA, although there was no significant difference as a function of ∑sulphide treatment, rates were generally higher at the 100 μM



14622920, 2020, 6, Downloaded from https://ami-journals.onlinelibrary.wiley.com/doi/10.1111/1462-2920.14969 by <Shibboleth>-member@library.princeton.edu, Wiley Online Library on [30/01/2024]. See the Terms and Conditions (https://onlinelibrary.wiley.com/terms-and-conditions) on Wiley Online Library for rules of use; OA articles are governed by the applicable Creative Commons License

**Table 1.** Statistical parameters describing the linear regression models of the change in $^{15}NH_4$, $^{29+30}N_2$, total $NH_4^+$, and $NO_x^-$ over time within each sulfide treatment.

| Sulphide Treatment | Model | Slope coefficient | Std. error | $R^2$ | *p*-value | *F* stat | Degrees of freedom |
|---|---|---|---|---|---|---|---|
| 0 μM | $^{15}NH_4^+$ ~ Time | 13.23 | 2.62 | 0.73 | 0.003 | 25.41 | 1 and 8 |
| | $^{29+30}N_2$ ~ Time | 30.37 | 0.89 | 0.99 | <0.001 | 1174 | 1 and 9 |
| | Total $NH_4^+$ ~ Time | 16.58 | 2.60 | 0.85 | <0.001 | 40.77 | 1 and 6 |
| | $NO_x^-$ ~ Time | −45.08 | 2.90 | 0.96 | <0.001 | 242.2 | 1 and 8 |
| 10 μM | $^{15}NH_4^+$ ~ Time | 11.95 | 3.33 | 0.52 | 0.005 | 12.89 | 1 and 10 |
| | $^{29+30}N_2$ ~ Time | 23.01 | 2.29 | 0.90 | <0.001 | 101.1 | 1 and 10 |
| | Total $NH_4^+$ ~ Time | 25.28 | 3.43 | 0.82 | <0.001 | 54.27 | 1 and 10 |
| | $NO_x^-$ ~ Time | −42.35 | 4.42 | 0.89 | <0.001 | 91.61 | 1 and 10 |
| 100 μM | $^{15}NH_4^+$ ~ Time | 23.18 | 2.55 | 0.89 | <0.001 | 82.75 | 1 and 9 |
| | $^{29+30}N_2$ ~ Time | 23.98 | 1.69 | 0.95 | <0.001 | 202.4 | 1 and 9 |
| | Total $NH_4^+$ ~ Time | 25.15 | 2.37 | 0.94 | <0.001 | 112.7 | 1 and 6 |
| | $NO_x^-$ ~ Time | −39.84 | 5.37 | 0.87 | <0.001 | 55.10 | 1 and 7 |
| 1000 μM | $^{15}NH_4^+$ ~ Time | 16.79 | 2.25 | 0.84 | <0.001 | 55.61 | 1 and 9 |
| | $^{29+30}N_2$ ~ Time | 10.02 | 1.68 | 0.79 | <0.001 | 35.5 | 1 and 8 |
| | Total $NH_4^+$ ~ Time | 28.64 | 3.31 | 0.88 | <0.001 | 74.91 | 1 and 9 |
| | $NO_x^-$ ~ Time | −40.84 | 5.53 | 0.84 | <0.001 | 54.46 | 1 and 9 |

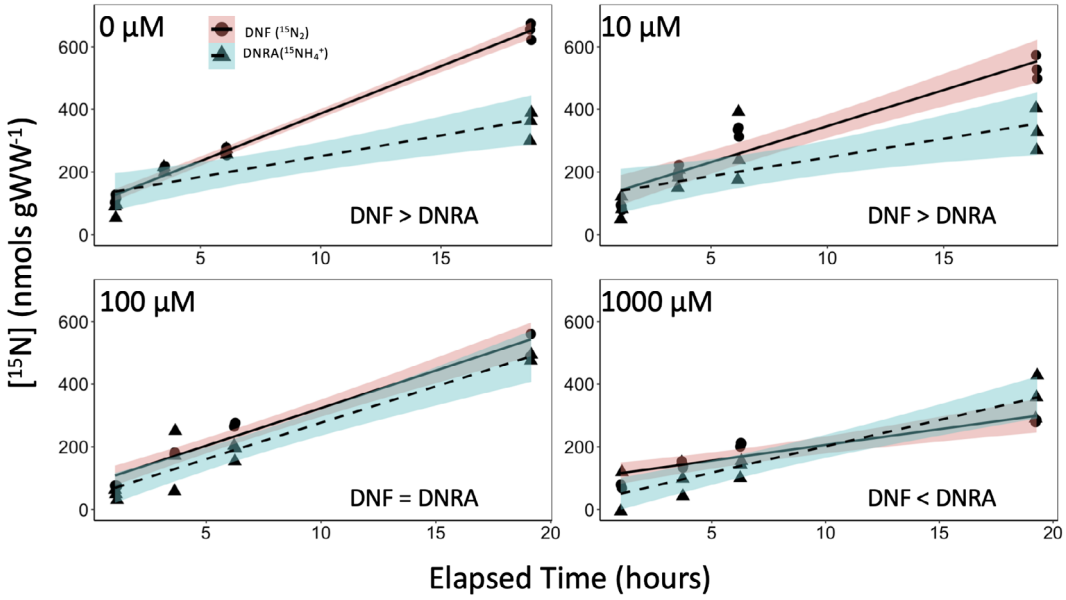


**Fig. 1.** The change in concentration (nmols g $WW^{-1}$) of 15NH4 (triangles) and $^{29+30}N_2$ (circles) over time across each sulphide treatment (0, 10, 100 and 1000 μM). Dashed and solid lines are the fitted linear models for $^{15}NH_4^+$ and $^{29+30}N_2$ respectively, with 95% confidence intervals represented by shading (red = $^{29+30}N_2$ ~ Elapsed Time, blue = $^{15}NH_4^+$ ~ Elapsed Time). A comparison of the rate of change between the two processes (DNRA indicated by change in 15NH4 and denitrification indicated by the change in $^{29+30}N_2$) was examined via ANCOVA and the relative importance of the two processes is provided in the corner of each panel. Linear regression statistical metrics are reported in Table 1. [Color figure can be viewed at wileyonlinelibrary.com]

**Table 2.** Average rates (standard errors) of nitrate consumption, total ammonium production, denitrification, and DNRA, as well as the amount of DNRA relative to denitrification, relative to total ammonium production, and relative to total nitrate reduction.

| | 0 μM | 10 μM | 100 μM | 1000 μM |
|---|---|---|---|---|
| Nitrate flux (nmol g $WW^{-1}$ $h^{-1}$) | −45.8 (4.2) | −42.4 (2.0) | −37.1 (5.2) | −38.9 (6.4) |
| Total Ammonium flux (nmol g $WW^{-1}$ $h^{-1}$) | 25.0 (1.4)$^a$ | 32.9 (1.8)$^{ab}$ | 39.2 (0.2)$^b$ | 36.2 (4.3)$^{ab}$ |
| Denitrification (nmol g $WW^{-1}$ $h^{-1}$) | 26.3 (0.6)$^a$ | 22.2 (1.2)$^{ac}$ | 20.0 (1.2)$^{bc}$ | 10.0 (0.4)$^d$ |
| DNRA (nmol g $WW^{-1}$ $h^{-1}$) | 13.5 (1.6) | 11.9 (3.7) | 24.0 (1.6) | 17.3 (3.1) |
| DNRA:Denitrification | 0.51 (0.06)$^a$ | 0.52 (0.14)$^a$ | 1.21 (0.09)$^{ab}$ | 1.73 (0.28)$^b$ |
| % DNRA of total $NH_4^+$ production | 54.8 (9.0)% | 37.3 (12.5)% | 57.2 (0.2)% | 48.5 (7.7)% |
| % DNRA of total $NO_3^-$ reduction | 33.6 (2.6)% | 33.3 (6.0)% | 54.5 (1.9)% | 62.7 (6.2)% |

Lower case letters represent significant differences across the sulphide treatments (ANOVA, Tukey posthoc tests).



14622920, 2020, 6, Downloaded from https://ami-journals.onlinelibrary.wiley.com/doi/10.1111/1462-2920.14969 by <Shibboleth>-member@library.princeton.edu, Wiley Online Library on [30/01/2024]. See the Terms and Conditions (https://onlinelibrary.wiley.com/terms-and-conditions) on Wiley Online Library for rules of use; OA articles are governed by the applicable Creative Commons License

treatment, which averaged 24.0 (±1.6) nmol g $WW^{-1}$ $h^{-1}$. The ratio of DNRA to complete denitrification was significantly higher in the 1000 μM ∑sulphide treatment, which averaged 1.73 (±0.28), compared with the 0 and 10 μM treatments, which averaged 0.51 (±0.6) and 0.52 (±0.14) respectively. DNRA contributed from 37.3 (±12.5)% to 57.2 (±0.2)% of total $NH_4^+$ production, with no significant difference across treatments. Finally, DNRA accounted for between 33.3 (±6.0)% in the 10 μM treatment and 62.7 (±6.2)% in the 1000 μM treatment of total dissimilatory $NO_x^-$ reduction (i.e. DNRA + denitrification), which generally increased with increasing ∑sulphide concentrations.

Rapid and dynamic changes in ∑sulphide levels were observed over the course of the time series across the treatments. The ∑sulphide concentrations ($H_2S$, $HS^-$ and $S^{2-}$) decreased rapidly within the first hour of the incubation in all the ∑sulphide treatments (Fig. S1). After 1 h, ∑sulphide concentrations averaged 365.0 (±93.8), 34.6 (±9.3) and 0.8 (±0.7) μM in the 1000, 100 and 10 μM treatments respectively. A more gradual decline was then observed through 6 h in the 100 and 1000 μM treatments. Between 6 and 18 h, ∑sulphide concentrations increased slightly in the 100 and 10 μM treatments, to 11.9 (±6.0) and 3.2 (±1.9) μM respectively; while in the 1000 μM treatment, concentrations continued to decrease, reaching 91.1 (±7.6) μM after 18 h. In the 0 μM treatment, ∑sulphide levels generally remained low (below 3.0 μM) across all replicates and time points, although in one replicate ∑sulphide concentrations peaked at 9.1 μM after the first hour but then dropped to 0 (Fig. S1).

The cumulative accumulation of $^{15}NH_4^+$ and $^{29+30}N_2$ and the cumulative consumption of $NO_x^-$ over the incubation were calculated by summing the total moles produced or consumed between each sampled time point multiplied by the number of hours elapsed within the respective time windows. Similar to the ratio of DNRA to complete denitrification rates (Table 2), the cumulative production of $^{15}NH_4^+$ (DNRA) relative to $^{29+30}N_2$ (denitrification) over the 18 h incubation generally increased with increasing ∑sulphide concentrations, with a significantly higher ratio at the 1000 μM ∑sulphide treatment compared with the other treatments (Fig. 2A). The cumulative production of $^{29+30}N_2$ generally decreased with increasing ∑sulphide concentrations, while there was no significant effect of ∑sulphide concentration on the cumulative production of $^{15}NH_4^+$ (Fig. 2B). The difference between the total $NO_x^-$ consumed compared with the $^{29+30}N_2$ plus $^{15}NH_4^+$ produced over the course of the incubation generally decreased with increasing ∑sulphide concentrations. In the 1000 μM ∑sulphide treatment there was notably more $NO_x^-$ consumed compared with $^{29+30}N_2$ plus $^{15}NH_4^+$ produced, suggesting an end-product that was not measured (e.g. $N_2O$, intracellular $NO_x^-$storage, or $NO_x^-$ assimilation into biomass) (Fig. 2B).

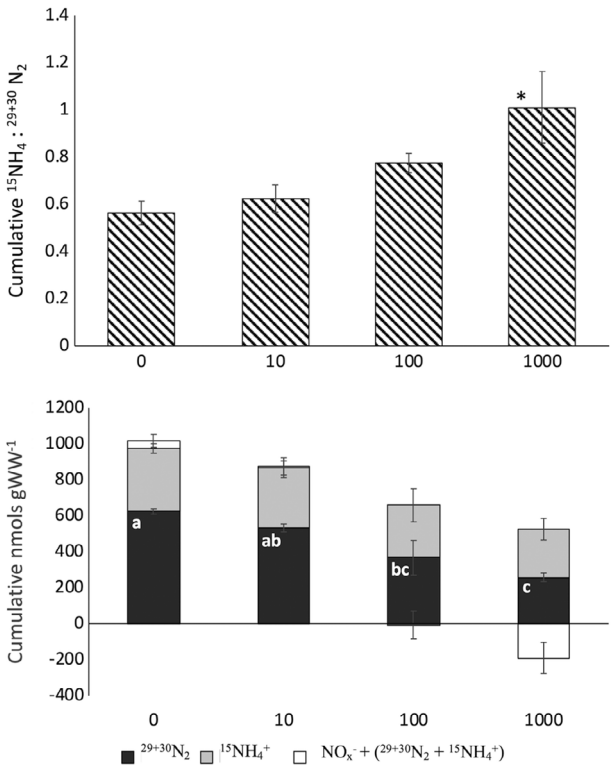


**Fig. 2.** The ratio of the cumulative production of $^{15}NH_4^+$ relative to $^{29+30}N_2$ over the 18-h incubation across the four sulphide treatments (top). The mass balance (white) of the cumulative consumption of $NO_x^-$ with the sum of the cumulative productions of $^{15}NH_4$ (light grey) and $^{29+30}N_2$ (dark grey) (bottom). A negative balance indicates $NO_x^-$ consumption exceeds production of $^{15}NH_4$+ and $^{29+30}N_2$ (i.e. 1000 μM). Letters represent significant differences across sulphide treatments for cumulative $^{29+30}N_2$ ($F(3,8) = 10.18$, $p$-value = 0.004). There was no significant effect of sulphide treatment on cumulative $^{15}NH_4$+ or the mass balance. Error bars are standard errors. [Color figure can be viewed at wileyonlinelibrary.com]

### *Bacterial communities*

At 1-, 6- and 18-h, the microbial communities across all ∑sulphide treatments and triplicates were characterized using a high-throughput 16S rRNA gene and 16S rRNA transcript amplicon sequencing. After quality filtering, clustering and removing chimeric sequences a total of 1 118 704 high-quality reads were retained across the 53 samples, which included both the 16S rRNA gene and 16S rRNA transcript datasets. Sequencing depth averaged 21 107 ± 1913 reads across all samples. After removing chloroplasts (0%–12.8%), mitochondria (0%–0.7%) and archaea (0%–1.9%), a total of 4952 amplicon sequence variants (ASVs) were retained across both the 16S rRNA gene and transcript datasets. The microbial communities' transcripts were significantly less diverse than the total microbial communities present (16S rRNA gene) (Shannon diversity index, ANOVA, $F_{1,50} = 51.6$, $p < 0.001$) (Fig. 3, Fig. S2). However, the microbial community transcript (16S rRNA transcript) diversity increased



14622920, 2020, 6, Downloaded from https://ami-journals.onlinelibrary.wiley.com/doi/10.1111/1462-2920.14969 by <Shibboleth>-member@library.princeton.edu, Wiley Online Library on [30/01/2024]. See the Terms and Conditions (https://onlinelibrary.wiley.com/terms-and-conditions) on Wiley Online Library for rules of use; OA articles are governed by the applicable Creative Commons License

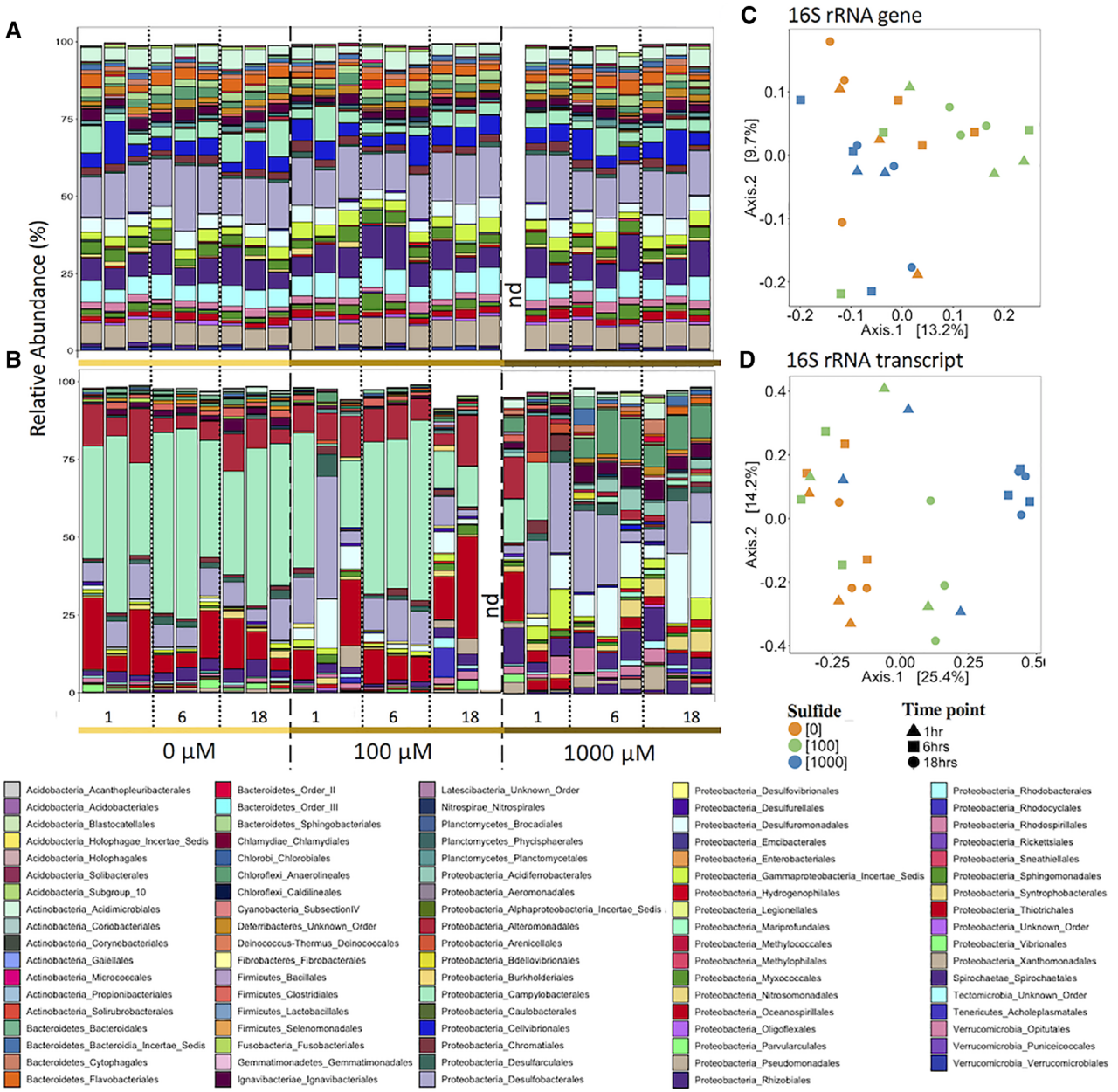


**Fig. 3.** Stacked bar plots showing taxonomic classification at the order level for the 16S rRNA gene (DNA) (A) and the 16S rRNA transcript (RNA) (B). Samples are organized by time point (1, 6 and 18 h) and sulphide treatment (0, 100 and 1000 µM). Data were rarefied to an equal sampling depth across both datasets ($n$ = 7878), relative abundance was calculated within each sample, and ASVs that composed less than 0.1% relative abundance across the two datasets were removed. ASVs were conglomerated within order, thus each bar does not represent an ASV but rather an entire order. Principal component analyses of the distance matrix of the 16SrRNA gene (C) and 16SrRNA transcript (D) dataset constructed with Bray–Curtis dissimilarity. Colours represent sulphide treatments and shapes correspond to time points. There was a significant effect of sulphide treatment but not time on the community structure across samples for both the 16SrRNA gene and 16SrRNA transcript (PERMANOVA, 16SrRNA gene: $F_{2,23}$ = 1.55, $p$ = 0.002; 16SrRNA transcript: $F_{2,24}$ = 3.48, $p$ = 0.001). nd = no data. [Color figure can be viewed at wileyonlinelibrary.com]

as a function of ∑sulphide (Shannon diversity index, ANOVA, $F_{2,23}$ = 27.6, $p$ < 0.001) (Fig. 3, Fig. S2).

The total bacterial communities (16S rRNA gene) across treatments and time points were generally unchanged and composed predominantly of members classified in the orders Acidimicrobiales (2.4%–6.2%), Cellvibrionales (3.0%–13.8%), Campylobacterales (2.1%–11.4%), Desulfobacterales (10.5%–20.4%), Rhizobiales (4.6%–14.0%), Rhodobacterales (3.5%–9.0%) and Xanthomonadales (5.2%–10.5%) (Fig. 3A). Despite appearing relatively static across ∑sulphide treatments, the total community structure was significantly affected by ∑sulphide concentration [Fig. 3C; 16SrRNA gene; permutational multivariate analysis of



14622920, 2020, 6, Downloaded from https://ami-journals.onlinelibrary.wiley.com/doi/10.1111/1462-2920.14969 by <Shibboleth>-member@library.princeton.edu, Wiley Online Library on [30/01/2024]. See the Terms and Conditions (https://onlinelibrary.wiley.com/terms-and-conditions) on Wiley Online Library for rules of use; OA articles are governed by the applicable Creative Commons License

variance (PERMANOVA), $F_{2,23} = p = 0.002$], while we did not detect an effect of incubation time. However, DESeq2 analysis revealed only a single ASV that was significantly differentially abundant across ∑sulphide treatments (p-adjusted <0.05; $log_2$-fold change of 6.9 between 0 and 100 μM; $log_2$-fold change of 7.0 between 1000 and 100 μM), which was most closely related to an isolated $SO_4^{2-}$ reducer, *Desulfofaba fastidiosa* [95.9% identity, NCBI's nucleotide collection database (Agarwala *et al*., 2018)], from the order Desulfobacterales (Abildgaard *et al*., 2004). This taxon was absent in all the 100 μM samples and was a very small component of the 0 and 1000 μM communities, averaging 0.27 ± 0.01% and 0.28 ± 0.04% relative abundance respectively.

In contrast to the total bacterial communities (16S rRNA gene), there were noticeable shifts in the actively transcribing bacterial communities (16S rRNA transcript) (Fig. 2B). The actively transcribing bacterial communities were significantly affected by ∑sulphide concentration (PERMANOVA, $F_{2,22} = 3.47$, $p = 0.001$) and time (PERMANOVA, $F_{2,22} = 1.53$, $p = 0.05$) (Fig. 3D). The actively transcribing bacterial communities associated with the 1000 μM ∑sulphide treatment were significantly more diverse and the ASVs were more evenly distributed compared with the 0 and 100 μM actively transcribing bacterial communities (Shannon diversity index, ANOVA $F_{2,23,\ =}$ 27.6, $p < 0.001$; Fig. 2, Fig. S3). The 0 and 100 μM treatments were overwhelmingly dominated by members of the order Campylobacterales, which averaged 45.6 ± 3.9% and 31.9 ± 6.8% relative abundances respectively. These treatments also had high relative abundances of members of the orders Oceanospirillales (0 μM averaged 11.4 ± 2.6%; 100 μM averaged 12.5 ± 3.0%) and Alteromonadales (0 μM averaged 8.7 ± 1.6; 100 μM averaged 9.8 ± 1.2%), orders that were generally lower in the 1000 μM treatment, particularly after 6 and 18 h. Instead, the 1000 μM treatment had high relative abundances of members of Anaerolineales (7.6 ± 1.7%), Desulfobacterales (15.4 ± 3.6%), Desulfuromonadales (10.8 ± 2.7%) and Rhizobiales (6.6 ± 1.2%).

Within the actively transcribing bacterial communities, the number of differentially abundant ASVs and the contribution of these ASVs to the actively transcribing communities across ∑sulphide treatments generally increased after the initial hour (Fig. S3, Supplemental Table). After 1 h, only 16 ASVs were significantly different across the three ∑sulphide treatments, making up between 1.4% and 15% of the active communities. After 6 h, 92 ASVs were significantly different by treatment, making up between 9.6% and 59% of the active communities. Finally, after 18 h, there were 89 significantly different ASVs, which ranged from 6.3% to 36.4% of the active communities (Fig. S3, Supplemental Table). The taxonomic classifications and the $log_2$-fold change values for all the ASVs (155 total) that were found to be significantly different within each time point across ∑sulphide treatments are provided in the Supplemental Table. Of these 155 ASVs, 57 changed by more than 4.3-fold (i.e. $log_2$-fold change >20 or $log_2$-fold change < −20), as visualized in Fig. S4.

Of the ASVs that were identified as significantly different across ∑sulphide treatments, members of the classes Anaerolineae, Deltaproteobacteria, Epsilonproteobacteria and Gammaproteobacteria made up considerable proportions of the actively transcribing communities (Fig. 4, Fig. S4). In general, within these groups, there were particular ASVs that were more active under sulphidic conditions, others that preferred low to no ∑sulphide concentrations, and a few that appeared to be more active in both the no ∑sulphide and the high ∑sulphide treatments as summarized in Fig. 4 and Fig. S4 and the conceptual diagram (Fig. 5). For example, Deltaproteobacteria including Desulfobulbaceae, Desulfobacteraceae, Desulfuromonadaceae and Geobacteraceae all responded positively to ∑sulphide concentrations. Additionally, members of Anaerolineaceae, Acidiferrobacteraceae and Xanthomonadales were significantly more active in the 1000 μM treatment. In contrast, Epsilonproteobacteria, including Campylobacteraceae and Helicobacteraceae, as well as some Gammaproteobacteria (i.e. Oceanospirillales and Alteromonadales) preferred low to no ∑sulphide conditions.

## Discussion

### *Sulphide alters the fate of $NO_x^-$*

Sulphide resulted in a significant shift in the relative contribution of DNRA and complete denitrification to total $NO_x^-$ reduction, ultimately promoting more bioavailable N retention as $NH_4^+$ compared with N loss through $N_2$ production (Figs 1 and 2; Table 2). The 100 and 1000 μM ∑sulphide treatments had generally higher rates of DNRA than the low ∑sulphide treatments (0 and 10 μM). Additionally, complete denitrification (i.e. $N_2$ production) significantly decreased with increasing ∑sulphide concentrations (Table 2). Several previous studies have reported similar observations, attributing a decrease in denitrification and either an increase or no difference in DNRA to high ∑sulphide (Brunet and Garcia-Gil, 1996; Bonaglia *et al*., 2016). ∑Sulphide may interact with the N cycle through a number of mechanisms. For example, studies have shown reduced sulphur directly inhibits denitrification (e.g. Sorensen *et al*., 1980; Jensen and Cox, 1992) while acting as a reductant (electron donor) for DNRA (e.g. Brunet and Garcia-Gil, 1996; An and Gardner, 2002). Thus, ∑sulphide has the potential to facilitate bioavailable N retention over removal.



14622920, 2020, 6, Downloaded from https://ami-journals.onlinelibrary.wiley.com/doi/10.1111/1462-2920.14969 by <Shibboleth>-member@library.princeton.edu, Wiley Online Library on [30/01/2024]. See the Terms and Conditions (https://onlinelibrary.wiley.com/terms-and-conditions) on Wiley Online Library for rules of use; OA articles are governed by the applicable Creative Commons License

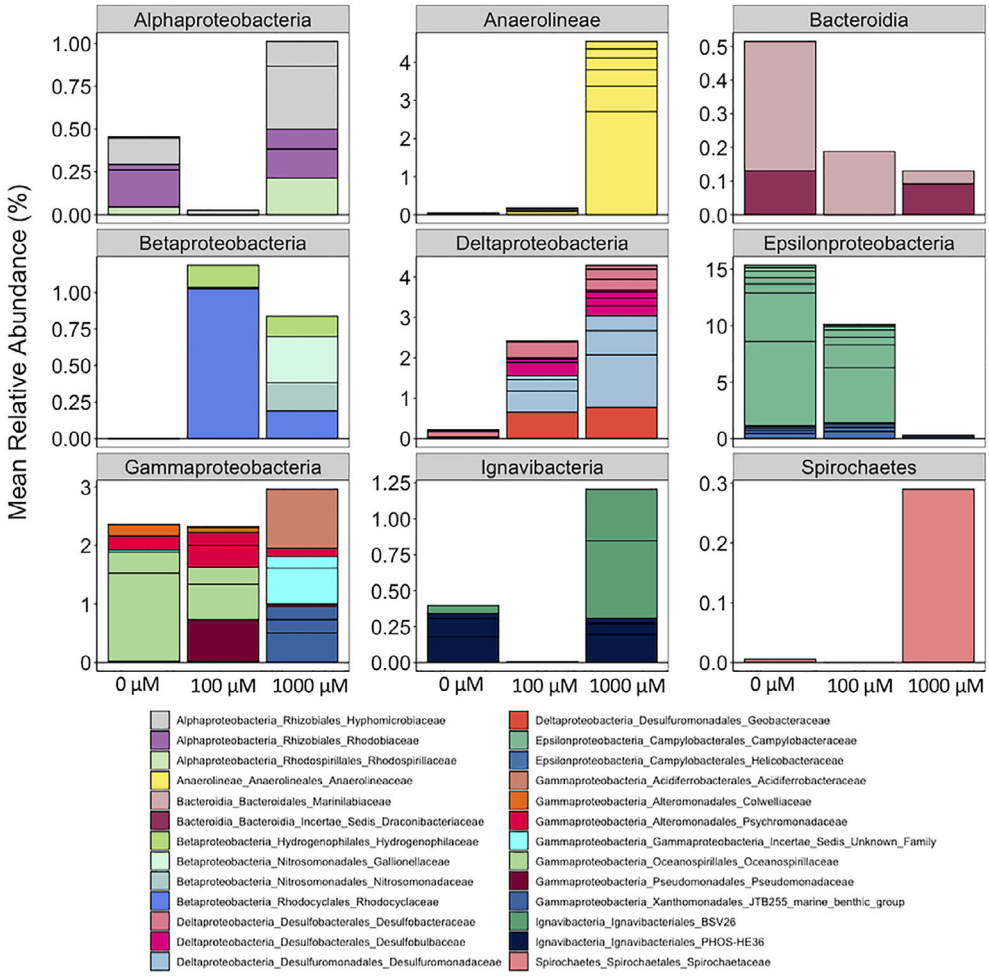


**Fig. 4.** Mean relative abundances of the differentially abundant ASVs (DESeq2, *p* adjusted <0.05) across sulphide treatments within the active bacterial communities (16SrRNA transcript); includes only ASVs with mean relative abundances that sum to >0.2% across all samples (i.e. 60 out of 155 differentially abundant ASVs). Data are faceted by Phylum and coloured by Family. [Color figure can be viewed at wileyonlinelibrary.com]

Typically, the relative contribution of DNRA and denitrification to total dissimilatory nitrate reduction is often correlated with the ratio of nitrate to organic carbon availability, with a higher ratio leading to denitrification as the dominant pathway (Tiedje, 1983; Algar and Vallino, 2014; Kraft *et al*., 2014; Hardison *et al*., 2015). In our experiment, we can assume this ratio was relatively consistent across ∑sulphide treatments, at least at the beginning of the incubation. Nitrate was experimentally provided in excess (100 µM) and was not completely depleted in any of the treatments by the end of the incubation (data not shown). The organic carbon profile and amount were consistent across treatments as the sediments were sourced from the same salt marsh sample and no organic carbon was added. However, despite the relatively consistent ratio of nitrate to organic carbon across treatments, the ratio of DNRA to complete denitrification shifted from 0.51 in the 0 µM ∑sulphide treatment to 1.73 in the high ∑sulphide treatment. This highlights the importance of ∑sulphide concentrations on the partitioning of $NO_3^-$ between these two pathways. Perhaps a more accurate predictor for the fate of $NO_3^-$, as also suggested by Robertson and Thamdrup (2017), is the availability of $NO_3^-$ relative to the availability of electron donors, including inorganic substrates (e.g. ∑sulphide, $Fe^{2+}$), not merely biologically available organic carbon as has been tested and modelled in previous studies (e.g. Algar and Vallino, 2014; Hardison *et al*., 2015).

The mass balance of the experimentally added $^{15}NO_x^-$ suggests that $^{15}NH_4$ and $^{29+30}N_2$ were not the only fates of $^{15}NO_x^-$ in the high ∑sulphide treatment, as there was more $^{15}NO_x^-$ consumed than $^{15}NH_4$ and $^{29+30}N_2$ produced in this treatment (Fig. 1B). More specifically, the sum of $^{15}NH_4$ and $^{29+30}N_2$ produced accounted for an average of 105%, 100%, and 95% of the total $^{15}NO_x^-$



14622920, 2020, 6, Downloaded from https://ami-journals.onlinelibrary.wiley.com/doi/10.1111/1462-2920.14969 by <Shibboleth>-member@library.princeton.edu, Wiley Online Library on [30/01/2024]. See the Terms and Conditions (https://onlinelibrary.wiley.com/terms-and-conditions) on Wiley Online Library for rules of use; OA articles are governed by the applicable Creative Commons License

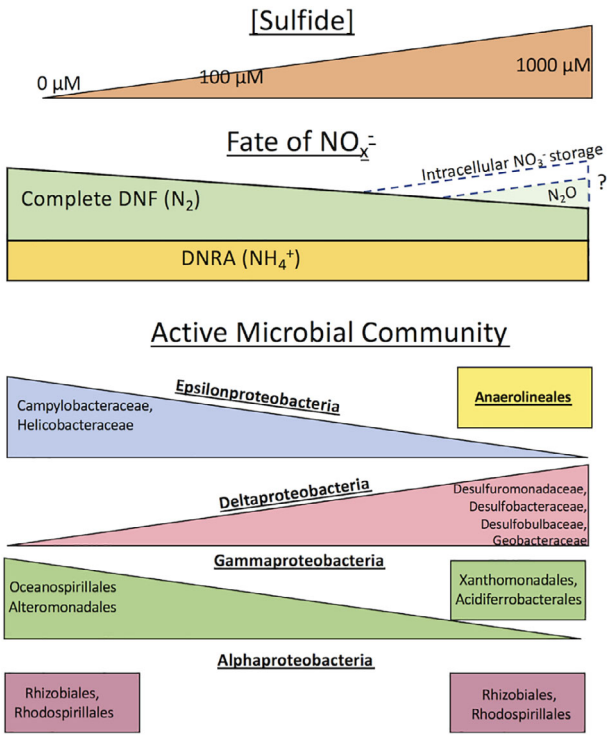


**Fig. 5.** Conceptual diagram depicting a synthesis of the general effects of increasing sulphide on the fates of nitrate ($NO_x^-$) and the relative abundances of the active bacterial community members. Dashed lines around intracellular $NO_3^-$ storage and $N_2O$ indicate these end-products were not directly measured in this study but inferred. General shifts in the active microbial community are organized and coloured by class. [Color figure can be viewed at wileyonlinelibrary.com]

consumed in the 0, 10 and 100 μM ∑sulphide treatments. However, in the 1000 μM treatment, the sum of the products $^{15}NH_4$ and $^{29+30}N_2$ only accounted for an average of 76% of the $^{15}NO_x^-$ consumed during the incubation. It is possible that the use of zinc chloride to preserve samples for $N_2$ analysis enhanced nitrous oxide in the sample due to interactions with $Fe^{2+}$ resulting in chemodenitrification (Ostrom *et al*., 2016; Buessecker *et al*., 2019). However, since zinc chloride was used across all treatments this effect would likely be consistent across treatments and may not be a valid explanation for the 'missing' N in the high ∑sulphide mass balance. There are three other possible alternative fates of $^{15}NO_x^-$ in the high ∑sulphide treatment, which were not measured in our study. One likely explanation is that high ∑sulphide concentrations inhibited the last step in denitrification ($N_2O$ to $N_2$), as previously shown (Sorensen *et al*., 1980; Senga *et al*., 2006; Aelion and Warttinger, 2009). This would result in an accumulation of $N_2O$ (e.g. Dalsgaard *et al*., 2013), an end-product that was not measured in our study, which has important implications as $N_2O$ is a potent greenhouse gas. A second possible fate of $^{15}NO_x^-$ is assimilation into microbial biomass. However, this is less likely given the high availability of $NH_4^+$ in the system, a preferable form of N for assimilation. Also, there is no reasonable explanation that high ∑sulphide would lead to greater $NO_x^-$ assimilation compared with low ∑sulphide conditions. Finally, another possible fate of $NO_x^-$ is the transport into and storage in intracellular $NO_3^-$ vacuoles (Fossing *et al*., 1995; Sayama, 2001; Zopfi *et al*., 2001). Accumulation of $^{15}NO_x^-$ in intracellular pools may have been promoted by sulphidic conditions in our experiment. There are numerous reports of nitrate-accumulating sulphur bacteria, (e.g. *Beggiatoa*, *Thiomargarita* and *Thioploca*) occurring in areas with high primary production, low dissolved oxygen and high soluble sulphide concentrations (McHatton *et al*., 1996; Schulz and Jørgensen, 2001). Some of these genera are classified as Thiotrichaceae (Teske *et al*., 1999), and we observed significantly higher abundances of Thiotrichaceae in the active community of the 1000 μM treatment at 18 h (Fig. 4). Many sulphur-oxidizing organisms that are capable of DNRA can also store $NO_x^-$ internally in vacuoles (Sayama, 2001; Zopfi *et al*., 2001; Sayama *et al*., 2005). Other nitrate-storing organisms include eukaryotes such as benthic microalgae (Kamp and Stief, 2017) and fungi (Shoun and Tanimoto, 1991; Zhou *et al*., 2002), which were not examined in our study but may play an important role in dictating the fate of nitrate. The breadth of microorganisms with the capacity to store $NO_3^-$ intracellularly is not entirely resolved and requires further investigation, however, most studies point to DNRA as the ultimate reduction pathway of the stored $NO_3^-$ (as reviewed in Kamp *et al*., 2015).

### *The total bacterial community was not strongly affected by ∑sulphide*

The total bacterial community (16S rRNA gene) did not differ substantially by ∑sulphide treatment nor did it shift over the course of the 18-h incubation; there are several possible explanations for this result including slow growth rates, potential dormancy and/or the presence of relic DNA. The total bacterial community structure and composition in our experiment was typical of salt marsh sediment communities (dominated by members of the classes Alphaproteobacteria (17.7%–23.6%), Deltaproteobacteria (19.8%–27.7%) and Gammaproteobacteria (18.9%–24.8%) (Fig. 3A) (e.g. Bowen *et al*., 2012; Angermeyer *et al*. 2016; Barreto *et al*. 2018). Owing to the heterogeneous environment of salt marsh sediments, both spatially and temporally, these microbial communities are adapted to rapid changes in ∑sulphide, nitrate and oxygen concentrations (Dini-Andreote *et al*. 2014, Kearns *et al*. 2016). This is reflected in high microbial diversity, extremely flexible metabolisms and high rates of dormancy observed in salt marsh microbial communities



14622920, 2020, 6, Downloaded from https://ami-journals.onlinelibrary.wiley.com/doi/10.1111/1462-2920.14969 by <Shibboleth>-member@library.princeton.edu, Wiley Online Library on [30/01/2024]. See the Terms and Conditions (https://onlinelibrary.wiley.com/terms-and-conditions) on Wiley Online Library for rules of use; OA articles are governed by the applicable Creative Commons License

(e.g. Fierer and Lennon, 2011; Lennon and Jones, 2011; Bowen *et al*., 2012; Kearns *et al*., 2016). A likely explanation for the lack of change observed in the DNA pool over the 18-h incubation is slow growth rates and DNA turnover rates associated with anaerobic metabolism. Biomass turnover is difficult to estimate and DNA turnover, even more challenging. However, it is typical for low energy environments dominated by anaerobic metabolism to exhibit slow biomass turnover, with estimates in the literature ranging from tens of days to thousands of years depending on the environment (e.g. Sundareshwar *et al*., 2003; Caffrey *et al*., 2007; Schmidt *et al*., 2007; Hoehler and Jorgensen, 2013). Thus, it is not surprising that we observed relatively little overall change in the total bacterial community under our experimental conditions over only 18 h. Instead, there was a significant difference in which community members were actively generating ribosomal RNA across the treatments and over the course of the incubation. As such, the total bacterial community structure and composition was not reflective of the actively transcribing bacterial community.

### *Sulphide promoted the activity of a more diverse bacterial community*

Unlike the total bacterial community, the active bacterial community was significantly affected by ∑sulphide concentration (Fig. 3B and D). Highly sulphidic conditions promoted the activity of a more diverse group of bacteria compared with the low and no ∑sulphide treatments, which became dominated by the activity of only a few particular groups (Fig. 2B). There are two possible explanations for this response: (i) ∑sulphide toxicity (Knowles, 1982; Schönharting *et al*., 1998) deterred the activity of these dominant members, allowing a more diverse group of bacteria to be active in the high ∑sulphide treatment, or (ii) the opposite, low or no ∑sulphide (and no $SO_4^{2-}$ in the artificial seawater) created a disturbance to these salt marsh communities, allowing only a select few members to dominate under low or no ∑sulphide conditions (and high nitrate). Saltmarsh microbial communities are typically exposed to ambient ∑sulphide concentrations upwards of 2000 μM (e.g. Thomas *et al*., 2014) and $SO_4^{2-}$ concentrations of full-strength seawater (~28 mM) (Howarth, 1984; Weston *et al*., 2006). Omitting ∑sulphide and $SO_4^{2-}$ may have resulted in the activity of select members of the total community, in particular, competitive nitrate-reducing organisms. For example, there were 20 ASVs, all classified as members of the genus Arcobacter (Campylobacteraceae) that were highly stimulated in the 0 and 100 μM treatments (Figs 3B and 4). These ASVs made up an average of 47.4% and 44.1% relative abundance of the active communities in the 0 and 100 μM treatments at 6 h respectively. Arcobacter are known denitrifiers that are promoted by high nitrate conditions (Heylen *et al*., 2006; Kraft *et al*., 2014; Saia *et al*., 2016), supporting the hypothesis that lower diversity in the low ∑sulphide treatments was due to the dominance of opportunistic organisms taking advantage of the high nitrate conditions. Interestingly, some of the Campylobacteraceae ASVs that we observed closely matched *Arcobacter nitrofigilis* [97%–99% identity, NCBI's nucleotide collection database (Agarwala *et al*., 2018)], a nitrogen fixer associated with the roots of *Spartina* plants (McClung *et al*., 1983). This organism has the capacity to reduce nitrate and produce ∑sulphide from cysteine (Pati *et al*., 2010), which may explain the slight increase in ∑sulphide concentrations in the low ∑sulphide treatments during the experiment.

### *Evidence of sulphide oxidation under high ∑sulphide*

Soluble sulphides can transform rapidly in salt marsh sediments by both biotic and abiotic pathways (Howarth, 1979; Howarth and Teal, 1979; Schippers and Jorgensen, 2002; Jørgensen *et al*., 2019). As such, in our experiment, the ∑sulphide treatments did not remain at targeted concentrations over the course of the incubation, and in fact, the added hydrogen sulphide decreased rapidly in the initial hour of the experiment (Fig. S1). This rapid depletion suggests the soluble sulphide likely reacted chemically with iron ($Fe^{2+}$) and/or iron oxides, which are generally high in salt marsh sediments (Kostka and Luther 1995, Tobias and Neubauer, 2009), ultimately producing iron monosulphides (FeS) and/or pyrite ($FeS_2$), which we did not measure in this experiment. When this reaction proceeds rapidly, small crystals are produced (Giblin, 1988) that have a high surface area to volume ratio making them readily available for microbial oxidation (Howarth, 1984; Bosch *et al*., 2012). Microbial oxidation of pyrite and soluble sulphides occurs using a variety of electron acceptors (e.g. oxygen, nitrate and iron) (Otte *et al*., 1999; Schippers and Jorgensen, 2002; Sayama *et al*., 2005). However, in this anoxic manipulation experiment, it is most likely that $NO_3^-$, which was provided in excess (100 μM), was used to oxidize the reduced sulphur (e.g. Cardoso *et al*., 2006; Tikhonova *et al*., 2006; Bosch *et al*., 2012). After the initial rapid depletion during the first hour, hydrogen ∑sulphide concentrations decreased more gradually over the next 6 h in the 100 and 1000 μM treatments (Fig. S1), potentially due to additional precipitation with iron and/or microbial transformations to oxidized forms (e.g. thiosulphate, sulphur monoxide and $SO_4^{2-}$). We did not measure these other sulphur species and thus cannot infer rates of ∑sulphide precipitation, ∑sulphide oxidation or $SO_4^{2-}$ reduction. However, important insight into sulphur cycling can be



14622920, 2020, 6, Downloaded from https://ami-journals.onlinelibrary.wiley.com/doi/10.1111/1462-2920.14969 by <Shibboleth>-member@library.princeton.edu, Wiley Online Library on [30/01/2024]. See the Terms and Conditions (https://onlinelibrary.wiley.com/terms-and-conditions) on Wiley Online Library for rules of use; OA articles are governed by the applicable Creative Commons License

gleaned from patterns in the active microbial communities across the ∑sulphide treatments.

In our study, there were some bacterial groups that exhibited a competitive advantage under high ∑sulphide conditions (i.e. higher abundances in the active community of the 1000 μM treatment compared with the 0 and 100 μM treatments) (Figs 3B and 4, Fig. S3). It is possible that some of these microorganisms can actively use reduced sulphur as an electron donor. For example, we observed nine ASVs classified in the family Desulfobulbaceae (Deltaproteobacteria) that were significantly more active under sulphidic conditions (adjusted *p*-value <0.05) (Supplemental Table, Fig. 4). Desulfobulbaceae include organisms known as cable bacteria that are capable of sulphur oxidation with either oxygen (Nielsen *et al*., 2010; Pfeffer *et al*., 2012) or nitrate (Marzocchi *et al*., 2014; Kessler *et al*., 2018, 2019) as electron acceptors. In addition to their role as sulphide oxidizers, a recent study showed cable bacteria enhanced the relative importance of DNRA by increasing $Fe^{2+}$ availability (via decreasing the pH which allowed FeS dissolution) that promoted other microbes in the community to conduct Fe-dependent DNRA (Kessler *et al*., 2019). However, in our experiment, only one Desulfobulbaceae ASV, that had no assigned Genus using the Silva database, closely matched a cable bacteria genus (Candidate genus *Electrothrix* (Trojan *et al*., 2016)] [>95% identity, NCBI's nucleotide collection database (Agarwala *et al*., 2018)]. Instead, the majority of the specific Desulfobulbaceae ASVs we observed were mostly classified under the genus Desulfobulbus. Desulfobulbus are known sulphate reducers, however, can also oxidize reduced sulphur (Fuseler *et al*., 1996), likely through the recently described enzymatic reversal of the sulphate reduction pathway (Thorup *et al*., 2017), and are closely related to the cable bacteria genera (Kjeldsen *et al*., 2019). A recent study revealed sulphate-reducing cellular machinery can function in reverse, allowing the potential for known sulphate reducers to be able to oxidize reduced sulphur species (Thorup *et al*., 2017), highlighting the challenge in deciphering function from taxonomic classification with 16S rRNA biomarker.

Aside from the increase in cable bacteria transcriptional activity, additional potential sulphide oxidizers were enhanced in the high ∑sulphide treatment. For example, seven ASVs classified as Acidiferrobacteraceae (Gammaproteobacteria) and four ASVs classified as Xanthomonadales were all significantly more active in the ∑sulphide treatments (Fig. 4, Figs S3 and S4, Supplemental Table). The Acidiferrobacteraceae ASVs most closely matched either *Sulfurifustis variabilis* (>96% identity) or *Sulfurifustis limicola* (>96% identity); the Xanthomonadales ASVs closely resembled *Sulfuriflexus mobilis* (>95% identity) [NCBI's nucleotide collection database (Agarwala *et al*., 2018)]. Recent sequencing of the complete genomes of all three of these organisms revealed them as chemolithotrophic sulphide oxidizers (Kojima *et al*., 2016; Umezawa *et al*., 2016; Watanabe *et al*., 2019). Although we acknowledge the limitations of using 16SrRNA transcript amplicon sequencing to infer the functional capacity of the active communities, given the biogeochemical data and the fact that these sequences are similar to known sulphide oxidizers, we are confident that sulphide oxidation was an important process in the ∑sulphide treatments. Our interpretation of the trends we observed in the microbial data is certainly limited by the tremendous gap in knowledge regarding the physiology and ecological roles of the taxonomies assigned to our 16S rRNA sequences. Further work using cultivation, physiology and metagenomic sequencing is required to fully understand the metabolic pathways associated with salt marsh microorganisms and the direct implications of these communities on biogeochemical cycling.

In addition to sulphide oxidizers, we observed an increase in the activity of potential $SO_4^{2-}$ reducing organisms in the 1000 μM ∑sulphide treatment, most of which are found within the Deltaproteobacteria class, including Desulfarculaceae (Suzuki *et al*., 2014), Desulfobacteraceae (Kuever, 2014) and Desulfuromonadaceae (Greene, 2014). In the high ∑sulphide treatment, the transformation of the reduced sulphur to oxidized states (e.g. $SO_4^{2-}$ and thiosulphate) could have subsequently fuelled these $SO_4^{2-}$ reducers, which are a prevalent and ecologically important functional group in ambient salt marsh sediments. Syntrophic relationships between sulphate reducers and sulphur-oxidizing microorganisms are likely important in these sulphidic sediments. In other environments, previous studies have reported tight interactions and syntrophy among these sulphur cycling functional groups (e.g. Lau *et al*., 2016).

## Conclusions

The availability of reduced sulphur species can exert an important control on the removal versus retention of bioavailable N within anaerobic sediments. Our results show ∑sulphide can have important implications for the fate of $NO_x^-$ in anaerobic systems, redirecting it away from $N_2$ and into other pools including $NH_4^+$, and potentially $N_2O$ and intracellular $NO_3^-$ pools. Furthermore, the observed shifts in the active bacterial communities in our controlled experiment suggest tight links between N and S cycling in salt marsh sediments. Numerous ASVs within Deltaproteobacteria, which include sulphate reducers and sulphur oxidizers, responded positively to high ∑sulphide concentrations. The interconnectedness and complexity of these elemental cycles, as well as the general lack of information on the physiology and metabolic



14622920, 2020, 6, Downloaded from https://ami-journals.onlinelibrary.wiley.com/doi/10.1111/1462-2920.14969 by <Shibboleth>-member@library.princeton.edu, Wiley Online Library on [30/01/2024]. See the Terms and Conditions (https://onlinelibrary.wiley.com/terms-and-conditions) on Wiley Online Library for rules of use; OA articles are governed by the applicable Creative Commons License

pathways of sediment microorganisms, pose a challenge in determining the mechanistic controls on N cycling. However, given the continued rise in the amount of reactive N delivered via rivers to the coastal zone coupled with increasing sea level rise that pushes $SO_4^{2-}$ laden seawater into tidal freshwater wetlands along those rivers, makes it essential that we use controlled experiments such as these to better understand the interactions between the sulphur and nitrogen cycles, and how they will change under future more sulphidic conditions.

## Experimental procedure

### *Sulphide manipulation experiment*

We conducted a sediment slurry, time-series experiment consisting of four $\sum$sulphide concentrations (0, 10, 100 and 1000 μM) (added as $Na_2S$ to anoxic water). Triplicate sediment cores were collected in July 2017 from the tall *Spartina alterniflora* ecotype in a salt marsh at the Plum Island Ecosystem Long-Term Ecological Research site in Rowley, MA (42.759 N, 70.891 W). Over the course of a day in July 2017, the water column at the site of core collection ranged in salinity from 22.2 to 27.3, the temperature ranged from 23.1 to 27.7°C, and the pH averaged 7.25 (±0.002) (Weston, 2019). Although porewater was not sampled during our sample collection, ambient concentrations of porewater $NH_4^+$, $PO_4^{3-}$ and sulphide at a nearby salt marsh during July 2017 averaged 62.1, 5.5 and 216.7 μM respectively (Morris and Sundberg, 2019). The intact cores were transported to Northeastern University's nearby Marine Science Centre on ice. In the lab, we extruded the cores and homogenized the surface sediment (0–5 cm) across the core replicates in an anoxic glove bag. Still, under anoxic conditions, we added 5 g wet weight (WW) of homogenized sediment to each 160 ml glass serum vial. The vials were filled with anoxic artificial seawater (sparged with $N_2$ gas), made without $SO_4^{2-}$, and spiked with $^{15}NO_3^-$, to achieve a concentration of 100 μM. The artificial seawater, which targeted a salinity and pH of 40 and 7 respectively, was made with the following: NaCl (27.72 g), KCl (0.67 g), $CaCl_2{\cdot}2H_2O$ (1.36 g), $MgCl_2$ (9.32 g), $NaHCO_3$ (0.18 g) into 1 l of Milli-Q water; this was then diluted to a salinity of 35, sparged with $N_2$ gas and spiked with $^{15}NO_3^-$. After adding the artificial seawater, the experimental vials were crimped with rubber septa ensuring no headspace. At 1, 3, 6 and 18 h, three vials from each $\sum$sulphide treatment were sacrificed and sampled. The vials were opened in the glove bag and the overlying water was sampled for $\sum$sulphide, $NO_2^-$ plus $NO_3^-$ ($NO_x^-$), $NH_4^+$, $^{29+30}N_2$ and $^{15}NH_4^+$. Sediments were subsampled into cryogenic vials (2 ml) and immediately flash-frozen in liquid nitrogen for downstream microbial analyses.

### *Analytical measurements*

Samples collected for $\sum$sulphide ($H_2S$, $HS^-$ and $S^{2-}$) analysis were preserved in zinc acetate and analysed within 1 week, colorimetrically following methods described in Cline (1969). We collected samples for $^{29+30}N_2$ analysis in 12 ml exetainers with no headspace, preserved them with $ZnCl_2$ (100 μl of 7 M stock), and stored them at 4°C until analysis within 2 weeks on a membrane inlet mass spectrometer (MIMS) with an in-line copper column furnace (Kana *et al*., 1994). Samples for dissolved concentrations of $NH_4^+$ and $NO_x^-$ were filtered (0.7 μm, glass fibre filters) and frozen until analysis. $NO_x^-$ samples were analysed via chemiluminescence on a Teledyne T200 NOx analyser (Teledyne API, San Diego, CA) following methods outlined in Cox (1980). Total $NH_4^+$ samples were analysed colorimetrically on a spectrophotometer following protocols from Solorzano (1969). $^{15}NH_4^+$ was analysed using the OX/MIMS method (Yin *et al*., 2014). Briefly, we thawed and sparged samples with helium to remove any residual $^{29+30}N_2$. Next, the samples were transferred to 12 ml exetainers, with no headspace, and spiked with 200 μl of hypobromite solution, which oxidizes $NH_4^+$ to $N_2$. After the addition of hypobromite, the samples were immediately capped, and the precipitate was allowed to settle overnight prior to analysing them on the MIMS for $^{29+30}N_2$. We calculated hourly rates of DNRA and denitrification as the change in $^{15}NH_4^+$ and $^{29+30}N_2$ over time respectively. Similarly, rates of $NO_x^-$ consumption and total $NH_4^+$ production were calculated as the change in concentration over time. We calculated the cumulative production of $^{29+30}N_2$, $^{15}NH4^+$ and total $NH_4^+$ and the cumulative consumption of $NO_x^-$ over the 18 h incubation by calculating the total moles produced or consumed between each sampled time point, multiplying by the number of hours elapsed within the respective time windows, and summing these values. We then constructed a mass balance for each $\sum$sulphide treatment as the cumulative consumption of $NO_x^-$ plus the cumulative productions of $^{15}NH_4^+$ and $^{29+30}N_2$.

### *16S rRNA gene and transcript library preparation*

DNA was extracted from ~0.25 g of sediment using the DNeasy Power Soil Extraction Kit (Qiagen, Valencia, CA). RNA was extracted using a modified version of Mettel and colleagues (2010) and described in detail in Kearns and colleagues (2016). RNA extracts were treated with DNase I (New England Biolabs, Ipswich, MA) following the manufacturer's protocol to remove any



14622920, 2020, 6, Downloaded from https://ami-journals.onlinelibrary.wiley.com/doi/10.1111/1462-2920.14969 by <Shibboleth>-member@library.princeton.edu, Wiley Online Library on [30/01/2024]. See the Terms and Conditions (https://onlinelibrary.wiley.com/terms-and-conditions) on Wiley Online Library for rules of use; OA articles are governed by the applicable Creative Commons License

DNA contamination. RNA was then reverse transcribed to cDNA using the Invitrogen Superscript RT III cDNA synthesis kit following the manufacturer's protocol. The V4 region of the 16S rRNA gene and transcript were amplified in triplicate reactions following the Earth Microbiome Project protocol using the 515F and 806R primers (Caporaso *et al*., 2011). The reverse primers included unique barcode sequences, which enable multiplexing samples on a single sequencing run. Amplicon libraries and negative PCR controls were checked on a gel to ensure amplicons matched the targeted size and that there was no contamination. The amplicons were size selected by gel excising followed by purification using the Qiagen QIAquick gel extraction kit (Qiagen). Libraries were quantified fluorometrically with the Qubit 3.0 (Life Technologies, Thermo Fisher Scientific, Waltham, MA) and pooled at equal molar concentrations per sample for sequencing on an Illumina MiSeq platform using the paired-end 250-cycle kit and V2 chemistry (Illumina, San Diego, CA). Sequencing was conducted at the University of Massachusetts Boston. All sequences have been deposited in the Sequence Read Archive under accession number PRJNA610907.

### *Bioinformatics analyses*

We demultiplexed raw reads using Illumina-utils (Eren *et al*., 2013) and we used the DADA2 (v1.7.0) workflow, implemented in R Studio (v3.4.1), to quality filter, merge paired-end reads, remove chimeric sequences, cluster sequences into ASVs and assign taxonomy against the Silva database (version 132) (Callahan *et al*., 2016; Callahan, 2018; Glöckner, 2019). Default parameters were used for all steps in the workflow. ASVs classified as archaea, mitochondria and chloroplast were removed from the dataset due to known primer biases and to focus the analyses specifically on the bacterial communities. Downstream data processing and statistical analyses were conducted using the Phyloseq package (v1.23.1) (McMurdie and Holmes, 2013) in R (R Core Team, 2019).

### *Statistical approach*

We assessed the change in $^{15}NH_4^+$, $^{29+30}N_2$, total $NH_4^+$ ($^{14+15}NH_4^+$) and $NO_x^-$ over time using linear models. Differences in the rates of denitrification, DNRA, total $NH_4^+$ flux, $NO_x^-$ flux and the ratio between DNRA and denitrification across the four $\sum$sulphide treatments were assessed with one-way analysis of variance (ANOVA) followed by Tukey post hoc analyses, when significant differences were determined. To compare rates of denitrification and DNRA within each $\sum$sulphide treatment, the change in $^{15}NH_4^+$ and $^{29+30}N_2$ over time were compared using analysis of covariance (ANCOVA). The effect of $\sum$sulphide concentration on the ratio of the cumulative production of $^{15}NH_4^+$ relative to $^{29+30}N_2$ was assessed using a one-way ANOVA. All data were tested for normality and homogeneity of variance using the Shapiro–Wilk test and Levene's test respectively.

We calculated Shannon diversity estimates on an ASV table rarefied to an even sequencing depth ($n$ = 7878). ANOVA was used to compare average Shannon diversity estimates between total (16S rRNA gene) and active (16S rRNA transcript) bacterial communities as well as across $\sum$sulphide treatments. Again, we used Shapiro–Wilk test and Levene's test to evaluate the assumptions of the ANOVA test.

To assess and compare the overall composition of the total (16S rRNA gene) and active (16S rRNA transcript) bacterial communities at each time point and across $\sum$sulphide treatments, we calculated Bray–Curtis dissimilarity using normalized (i.e. percent relative abundance) ASV tables. Bray–Curtis dissimilarities were ordinated using Principal Coordinates Analysis. After testing for homogeneity of multivariate dispersions, using betadisper in the vegan package (v2.5.4), we assessed the statistical differences in bacterial community compositions as a function of elapsed time and across $\sum$sulphide treatments using PERMANOVA implemented using adonis in the vegan package (v2.5.4). We also conducted pairwise comparisons within each time point (1, 6 and 18 h) across $\sum$sulphide concentrations (0, 100 and 1000 μM) using DESeq2 (v1.22.2) to determine the ASVs that were significantly different in abundances across $\sum$sulphide treatments at each time point (Benjamini–Hochberg adjusted $p$-value <0.05) (Love *et al*., 2014).

## Acknowledgements

We are grateful to Michael Greenwood and Christopher Lynum for analytical support in the lab. This work was funded in part by a grant awarded to J.L.B. (NSF CAREER DEB1350491).

## References

Abildgaard, L., Ramsing, N.B., and Finster, K. (2004) Characterization of the marine propionate-degrading, sulfate-reducing bacterium *Desulfofaba fastidiosa* sp. nov. and reclassification of *Desulfomusa hansenii* as *Desulfofaba hansenii* comb. nov. *Int J Syst Evol Microbiol* **54**: 393–399.

Aelion, C.M., and Warttinger, U. (2009) Low $\sum$sulfide concentrations affect nitrate transformations in freshwater and saline coastal retention pond sediments. *Soil Biol Biochem* **41**: 735–741.

Agarwala, R., Barrett, T., Beck, J., Benson, D.A., Bollin, C., Bolton, E., *et al*. (2018) Database resources of the National Center for Biotechnology Information. *Nucleic Acids Res* **44**: D7–D19.



14622920, 2020, 6, Downloaded from https://ami-journals.onlinelibrary.wiley.com/doi/10.1111/1462-2920.14969 by <Shibboleth>-member@library.princeton.edu, Wiley Online Library on [30/01/2024]. See the Terms and Conditions (https://onlinelibrary.wiley.com/terms-and-conditions) on Wiley Online Library for rules of use; OA articles are governed by the applicable Creative Commons License

Algar, C.K., and Vallino, J.J. (2014) Predicting microbial nitrate reduction pathways in coastal sediments. *Aquat Microb Ecol* **71**: 223–238.

An, S., and Gardner, W.S. (2002) Dissimilatory nitrate reduction to ammonium (DNRA) as a nitrogen link, versus denitrification as a sink in a shallow estuary (Laguna Madre/Baffin Bay, Texas). *Mar Ecol Prog Ser* **237**: 41–50.

Angermeyer, A., Crosby, S.C., and Huber, J.A. (2016) Decoupled distance-decay patterns between dsrA and 16S rRNA genes among salt marsh sulfate-reducing bacteria. *Environ Microbiol* **18**: 75–86.

Barreto, C.R., Morrissey, E.M., Wykoff, D.D., and Chapman, S.K. (2018) Co-occurring mangroves and salt marshes differ in microbial community composition. *Wetlands* **38**: 497–508.

Bonaglia, S., Klawonn, I., De Brabandere, L., Deutsch, B., Thamdrup, B., and Brüchert, V. (2016) Denitrification and DNRA at the Baltic Sea oxic–anoxic interface: substrate spectrum and kinetics. *Limnol Oceanogr* **61**: 1900–1915.

Bosch, J., Lee, K.Y., Jordan, G., Kim, K.W., and Meckenstock, R.U. (2012) Anaerobic, nitrate-dependent oxidation of pyrite nanoparticles by *Thiobacillus denitrificans*. *Environ Sci Technol* **46**: 2095–2101.

Bowen, J.L., Morrison, H.G., Hobbie, J.E., and Sogin, M.L. (2012) Salt marsh sediment diversity: a test of the variability of the rare biosphere among environmental replicates. *ISME J* **6**: 2014–2023.

Bradley, P.M., and Dunn, E.L. (1989) Effects of ∑sulfide on the growth of three salt marsh halophytes of the southeastern United States. *Am J Bot* **76**: 1707–1713.

Brunet, R.C., and Garcia-Gil, L.J. (1996) ∑Sulfide-induced dissimilatory nitrate reduction to ammonia in anaerobic freshwater sediments. *FEMS Microbiol Ecol* **21**: 131–138.

Buessecker, S., Tylor, K., Nye, J., Holbert, K.E., Urquiza Munoz, J.D., Glass, J.B., *et al*. (2019) Effects of sterilization techniques on chemodenitrification and N2O production in tropical peat soil microcosms. *Biogeosciences* **16**: 4601–4612.

Bulseco, A.N., Giblin, A.E., Tucker, J., Murphy, A.E., Sanderman, J., Hiller-Bittrolff, K., and Bowen, J.L. (2019) Nitrate addition stimulates microbial decomposition of organic matter in salt marsh sediments. *Glob Chang Biol* **25**: 3224–3241.

Caffrey, J.M., Murrell, M.C., Wigand, C., and McKinney, R. (2007) Effect of nutrient loading on biogeochemical and microbial processes in a New England salt marsh. *Biogeochemistry* **82**: 251–264.

Callahan, B. (2018) Silva taxonomic training data formatted for DADA2 (Silva version 132). Zenodo.

Callahan, B.J., McMurdie, P.J., Rosen, M.J., Han, A.W., Johnson, A.J.A., and Holmes, S.P. (2016) DADA2: high-resolution sample inference from Illumina amplicon data. *Nat Methods* **13**: 581–583.

Caporaso, J.G., Lauber, C.L., Walters, W.A., Berg-Lyons, D., Lozupone, C.A., Turnbaugh, P.J., *et al*. (2011) Global patterns of 16S rRNA diversity at a depth of millions of sequences per sample. *Proc Natl Acad Sci U S A* **108**: 4516–4522.

Cardoso, R.B., Sierra-Alvarez, R., Rowlette, P., Flores, E.R., Gómez, J., and Field, J.A. (2006) ∑sulfide oxidation under chemolithoautotrophic denitrifying conditions. *Biotechnol Bioeng* **95**: 1148–1157.

Cline, J.D. (1969) Spectrophotometric determination of hydrogen ∑sulfide. *Limnol Oceanogr* **14**: 454–458.

Cox, R.D. (1980) Determination of nitrate and nitrite at the parts per billion level by chemiluminescence. *Anal Chem* **52**: 332–335.

Dalsgaard, T., De Brabandere, L., and Hall, P.O.J. (2013) Denitrification in the water column of the Central Baltic Sea. *Geochim Cosmochim Acta* **106**: 247–260.

Dini-Andreote, F., de Cássia Pereira e Silva, M., Triadó-Margarit, X., Casamayor, E.O., van Elsas, J.D., and Salles, J.F. (2014) Dynamics of bacterial community succession in a salt marsh chronosequence: evidences for temporal niche partitioning. *ISME* **J8**: 1989–2001. https://doi.org/10.1038/ismej.2014.54.

Eren, A.M., Vineis, J.H., Morrison, H.G., and Sogin, M.L. (2013) A filtering method to generate high quality short reads using Illumina paired-end technology. *PLoS One* **8** (6): e66643. https://doi.org/10.1371/journal.pone.0066643.

Fierer, N., and Lennon, J.T. (2011) The generation and maintenance of diversity in microbial communities. *Am J Bot* **98**: 439–448.

Fossing, H., Gallardo, V.A., Jorgensen, B.B., Huttel, M., Nielsen, L.P., Schulz, H., *et al*. (1995) Concentration and transport of nitrate by the mat-forming Sulphur bacterium Thioploca. *Nature* **374**: 713–715.

Fuseler, K., Krekeler, D., Sydow, U., and Cypionka, H. (1996) A common pathway of sulfide oxidation by sulfate-reducing bacteria. *FEMS Microbiol Lett* **144**: 129–134.

Giblin, A., Tobias, C., Song, B., Weston, N., Banta, G., and Rivera-Monroy, V. (2013) The importance of dissimilatory nitrate reduction to ammonium (DNRA) in the nitrogen cycle of coastal ecosystems. *Oceanography* **26**: 124–131.

Giblin, A.E. (1988) Pyrite formation in marshes during early diagenesis. *Geomicrobiol J* **6**: 77–97.

Glöckner, F.O. (2019) The SILVA database project: an ELIXIR core data resource for high-quality ribosomal RNA sequences. *Biodivers Inf Sci Stand* **3**: e36125.

Graves, C.J., Makrides, E.J., Schmidt, V.T., Giblin, A.E., Cardon, Z.G., and Rand, D.M. (2016) Functional responses of salt marsh microbial communities to long-term nutrient enrichment (G Voordouw, Ed.). *Appl Environ Microbiol* **82**: 2862–2871.

Greene, A.C. (2014) The family Desulfuromonadaceae. In *The Prokaryotes*, Rosenberg, E., DeLong, E.F., Lory, S., Stackebrandt, E., and Thompson, F. (eds). Berlin, Heidelberg, Germany: Springer.

Hannig, M., Lavik, G., Kuypers, M.M.M., Woebken, D., Martens-Habbena, W., and Jürgens, K. (2007) Shift from denitrification to anammox after inflow events in the Central Baltic Sea. *Limnol Oceanogr* **52**: 1336–1345.

Hardison, A.K., Algar, C.K., Giblin, A.E., and Rich, J.J. (2015) Influence of organic carbon and nitrate loading on partitioning between dissimilatory nitrate reduction to ammonium (DNRA) and N2 production. *Geochim Cosmochim Acta* **164**: 146–160.

Heylen, K., Verstraete, W., De Vos, P., Vanparys, B., Wittebolle, L., and Boon, N. (2006) Cultivation of denitrifying bacteria: optimization of isolation conditions



14622920, 2020, 6, Downloaded from https://ami-journals.onlinelibrary.wiley.com/doi/10.1111/1462-2920.14969 by <Shibboleth>-member@library.princeton.edu, Wiley Online Library on [30/01/2024]. See the Terms and Conditions (https://onlinelibrary.wiley.com/terms-and-conditions) on Wiley Online Library for rules of use; OA articles are governed by the applicable Creative Commons License

and diversity study. *Appl Environ Microbiol* **72**: 2637–2643.
Hietanen, S., Jäntti, H., Buizert, C., Jürgens, K., Labrenz, M., Voss, M., and Kuparinen, J. (2012) Hypoxia and nitrogen processing in the Baltic Sea water column. *Limnol Oceanogr* **57**: 325–337.
Hoehler, T.M., and Jorgensen, B.B. (2013) Microbial life under extreme energy limitation. *Nat Rev Microbiol* **11**: 83–94.
Howarth, R.W. (1979) Pyrite: its rapid formation in a salt marsh and its importance in ecosystem metabolism. *Science* **203**: 49–51.
Howarth, R.W. (1984) The ecological significance of sulfur in the energy dynamics of salt marsh and coastal marine sediments. *Biogeochemistry* **1**: 5–27.
Howarth, R.W., and Teal, J.M. (1979) Sulfate reduction. *Limnol Oceanogr* **24**: 999–1013.
Jensen, K.M., and Cox, R.P. (1992) Effects of ∑sulfide and low redox potential on the inhibition of nitrous oxide reduction by acetylene in Pseudomonas nautica. *FEMS Microbiol Lett* **96**: 13–18.
Jensen, M.M., Petersen, J., Dalsgaard, T., and Thamdrup, B. (2009) Pathways, rates, and regulation of N2 production in the chemocline of an anoxic basin, Mariager Fjord, Denmark. *Mar Chem* **113**: 102–113.
Jørgensen, B.B., Findlay, A.J., and Pellerin, A. (2019) The biogeochemical sulfur cycle of marine sediments. *Front Microbiol* **10**: 1–27.
Joye, S.B., and Hollibaugh, J.T. (1995) Influence of ∑sulfide inhibition of nitrification on nitrogen regeneration in sediments. *Science* **270**: 623–625.
Kamp, A., Hogslund, S., Risgaard-Petersen, N., and Stief, P. (2015) Nitrate storage and dissimilatory nitrate reduction by eukaryotic microbes. *Front Microbiol* **6**: 1–15.
Kamp, A., and Stief, P. (2017) Editorial: eukaryotic microbes store nitrate for "breathing" in anoxia. *Front Microbiol* **8**: 2439.
Kana, T.M., Darkangelo, C., Hunt, M.D., Oldham, J.B., Bennett, G.E., and Cornwell, J.C. (1994) Membrane inlet mass spectrometer for rapid high-precision determination of $N_2$, $O_2$, and Ar in environmental water samples. *Anal Chem* **66**: 4166–4170.
Kearns, P.J., Angell, J.H., Howard, E.M., Deegan, L.A., Stanley, R.H.R., and Bowen, J.L. (2016) Nutrient enrichment induces dormancy and decreases diversity of active bacteria in salt marsh sediments. *Nat Commun* **7**: 12881.
Kessler, A.J., Roberts, K.L., Bissett, A., and Cook, P.L.M. (2018) Biogeochemical controls on the relative importance of denitrification and dissimilatory nitrate reduction to ammonium in estuaries. *Glob Biogeochem Cycles* **32**: 1045–1057.
Kessler, A.J., Wawryk, M., Marzocchi, U., Roberts, K.L., Wong, W.W., Risgaard-Petersen, N., *et al*. (2019) Cable bacteria promote DNRA through iron ∑sulfide dissolution. *Limnol Oceanogr* **64**: 1228–1238.
Kjeldsen, K.U., Schreiber, L., Thorup, C.A., Boesen, T., Bjerg, J.T., Yang, T., *et al*. (2019) On the evolution and physiology of cable bacteria. *Proc Natl Acad Sci U S A* **116**: 19116–19125. https://doi.org/10.1073/pnas.1903514116.
Knowles, R. (1982) Denitrification. *Microbiol Rev* **46**: 43–70.
Kojima, H., Watanabe, T., and Fukui, M. (2016) Sulfuricaulis limicola gen. Nov., sp. nov., a sulphur oxidizer isolated from a lake. *Int J Syst Evol Microbiol* **66**: 266–270.
Kostka, J.E., and Luther, G.W. (1995) Seasonal cycling of Fe in saltmarsh sediments. *Biogeochemistry* **29**: 159–181. https://doi.org/10.1007/BF00000230.
Kraft, B., Tegetmeyer, H.E., Sharma, R., Klotz, M.G., Ferdelman, T.G., Hettich, R.L., *et al*. (2014) The environmental controls that govern the end product of bacterial nitrate respiration. *Science* **345**: 676–679.
Kuever, J. (2014) The family Desulfobacteraceae. In *The Prokaryotes*, Rosenberg, E., DeLong, E.F., Lory, S., Stackebrandt, E., and Thompson, F. (eds). Berlin, Heidelberg, Germany: Springer.
Lau, M.C.Y., Kieft, T.L., Kuloyo, O., Linage-Alvarez, B., Van Heerden, E., Lindsay, M.R., *et al*. (2016) An oligotrophic deep-subsurface community dependent on syntrophy is dominated by sulfur-driven autotrophic denitrifiers. *Proc Natl Acad Sci U S A* **113**: E7927–E7936.
Lennon, J.T., and Jones, S.E. (2011) Microbial seed banks: the ecological and evolutionary implications of dormancy. *Nat Rev Microbiol* **9**: 119–130.
Love, M. I., Anders, S., and Huber, W. (2014) DESeq2 package__Differential analysis of count data.
Mania, D., Heylen, K., van Spanning, R.J.M., and Frostegård, Å. (2014) The nitrate-ammonifying and nosZ-carrying bacterium *Bacillus vireti* is a potent source and sink for nitric and nitrous oxide under high nitrate conditions. *Environ Microbiol* **16**: 3196–3210.
Marzocchi, U., Trojan, D., Larsen, S., Meyer, R.L., Revsbech, N.P., Schramm, A., *et al*. (2014) Electric coupling between distant nitrate reduction and ∑sulfide oxidation in marine sediment. *ISME J* **8**: 1682–1690.
McClung, C.R., van Berkum, P., Davis, R.E., and Sloger, C. (1983) Enumeration and localization of N2-fixing bacteria associated with roots of *Spartina alterniflora* Loisel. *Appl Environ Microbiol* **45**: 1914–1920.
McHatton, S., Barry, J., Jannasch, H., and Nelson, D. (1996) High nitrate concentrations in vacuolate, autotrophic marine Beggiatoa spp. *Appl Environ Microbiol* **62**: 954–958.
McMurdie, P.J., and Holmes, S. (2013) Phyloseq: An R package for reproducible interactive analysis and graphics of microbiome census data. *PLoS One* **8**: e61217.
Mettel, C., Kim, Y., Shrestha, P.M., and Liesack, W. (2010) Extraction of mRNA from soil. *Appl Environ Microbiol* **76**: 5995–6000.
Morris, J., and Sundberg, K., 2019 Porewater nutrient concentrations from control plots at a *Spartina alterniflora*-dominated salt marsh at Law's Point, Rowley River, Plum Island Ecosystem LTER, MA. Environmental Data Initiative. URL http://dx.doi.org/10.6073/pasta/15a041cb5635fd061a29673be81daeeb.
Nielsen, L.P., Risgaard-Petersen, N., Fossing, H., Christensen, P.B., and Sayama, M. (2010) Electric currents couple spatially separated biogeochemical processes in marine sediment. *Nature* **463**: 1071–1074.
Nixon, S.W. (1995) Coastal marine eutrophication: a definition, social causes, and future concerns. *Ophelia* **41**: 199–219.
Ostrom, N.E., Gandhi, H., Trubl, G., and Murray, A.E. (2016) Chemodenitrification in the cyroecosystem of Lake Vida, Victoria Valley, Antarctica. *Geobiology* **14**: 575–587.



14622920, 2020, 6, Downloaded from https://ami-journals.onlinelibrary.wiley.com/doi/10.1111/1462-2920.14969 by <Shibboleth>-member@library.princeton.edu, Wiley Online Library on [30/01/2024]. See the Terms and Conditions (https://onlinelibrary.wiley.com/terms-and-conditions) on Wiley Online Library for rules of use; OA articles are governed by the applicable Creative Commons License

Otte, S., Nielsen, L.P., Paerl, H.W., Zopfi, J., Schulz, H.N., Teske, A., *et al*. (1999) Nitrogen, carbon, and sulfur metabolism in natural Thioploca samples. *Appl Environ Microbiol* **65**: 3148–3157.

Pati, A., Gronow, S., Lapidus, A., Copeland, A., del Rio, T. G., Nolan, M., *et al*. (2010) Complete genome sequence of Arcobacter nitrofigilis type strain (CI T). *Stand Genomic Sci* **2**: 300–308.

Pfeffer, C., Larsen, S., Song, J., Dong, M., Besenbacher, F., Meyer, R.L., *et al*. (2012) Filamentous bacteria transport electrons over centimetre distances. *Nature* **491**: 218–221.

R Core Team. (2019) *R: A Language and Environment for Statistical Computing*. Vienna, Austria: R Foundation for Statistical Computing.

Rey, J.R., Shaffer, J., Kain, T., Stahl, R., and Crossman, R. (1992) ∑Sulfide variation in the pore and surface waters of artificial salt-marsh ditches and a natural Tidal Creek. *Estuaries* **15**: 257–269.

Robertson, E.K., and Thamdrup, B. (2017) The fate of nitrogen is linked to iron(II) availability in a freshwater lake sediment. *Geochim Cosmochim Acta* **205**: 84–99. https://doi.org/10.1016/j.gca.2017.02.014.

Saia, F.T., Souza, T.S.O., Duarte, R.T.D., Pozzi, E., Fonseca, D., and Foresti, E. (2016) Microbial community in a pilot-scale bioreactor promoting anaerobic digestion and sulfur-driven denitrification for domestic sewage treatment. *Bioprocess Biosyst Eng* **39**: 341–352.

Sanford, R.A., Wagner, D.D., Wu, Q., Chee-Sanford, J.C., Thomas, S.H., Cruz-García, C., *et al*. (2012) Unexpected nondenitrifier nitrous oxide reductase gene diversity and abundance in soils. *Proc Natl Acad Sci U S A* **109**: 19709–19714.

Sayama, M. (2001) Presence of nitrate-accumulating sulfur bacteria and their influence on nitrogen cycling in a shallow coastal marine sediment. *Appl Environ Microbiol* **67**: 3481–3487.

Sayama, M., Risgaard-Petersen, N., Nielsen, L.P., Fossing, H., and Christensen, P.B. (2005) Impact of bacterial NO3-transport on sediment biogeochemistry. *Microbiology* **71**: 7575–7577.

Schippers, A., and Jorgensen, B.B. (2002) Biogeochemistry of pyrite and iron ∑sulfide oxidation in marine sediments. *Geochim Cosmochim Acta* **66**: 85–92.

Schmidt, S.K., Costello, E.K., Nemergut, D.R., Cleveland, C.C., Reed, S.C., Weintraub, M.N., *et al*. (2007) Biogeochemical consequences of rapid microbial turnover and seasonal succession in soil. *Ecology* **88**: 1379–1385.

Schönharting, B., Rehner, R., Metzger, J.W., Krauth, K., and Rizzi, M. (1998) Release of nitrous oxide (N2O) from denitrifying activated sludge caused by H2S-containing wastewater: quantification and application of a new mathematical model. *Water Sci Technol* **38**: 237–246.

Schulz, H.N., and Jørgensen, B.B. (2001) Big bacteria. *Annu Rev Microbiol* **55**: 105–137.

Senga, Y., Mochida, K., Fukumori, R., Okamoto, N., and Seike, Y. (2006) N2O accumulation in estuarine and coastal sediments: the influence of H2S on dissimilatory nitrate reduction. *Estuar Coast Shelf Sci* **67**: 231–238.

Shoun, H., and Tanimoto, T. (1991) Denitrification by the fungus Fusarium oxysporum and involvement of cytochrome P-450 in the respiratory nitrite reduction. *J Biol Chem* **266**: 11078–11082.

Solorzano, L. (1969) Determination of ammonia in natural waters by the phenolhypochlorite method. *Limnol Oceanogr* **14**: 799–801.

Sorensen, J., Tiedje, J.M., and Firestone, R.B. (1980) Inhibition by ∑sulfide of nitric and nitrous-oxide reduction by denitrifying Pseudomonas-fluorescens. *Appl Environ Microbiol* **39**: 105–108.

Sundareshwar, P.V., Morris, J.T., Koepfler, E.K., and Fornwalt, B. (2003) Phosphorus limitation of coastal ecosytem processes. *Science* **299**: 563–565.

Suzuki, D., Li, Z., Cui, X., Zhang, C., and Katayama, A. (2014) Reclassification of *Desulfobacterium anilini* as *Desulfatiglans anilini* comb. nov. within Desulfatiglans gen. nov., and description of a 4-chlorophenol-degrading sulfate-reducing bacterium, *Desulfatiglans parachlorophenolica* sp. nov. *Int J Syst Evol Microbiol* **64**: 3081–3086.

Teske, A., Sogin, M.L., Nielson, L.P., and Jannasch, H.W. (1999) Phylogenetic relationships of a large marine beggiatoa. *Syst Appl Microbiol* **22**: 39–44.

Thomas, F., Giblin, A.E., Cardon, Z.G., and Sievert, S.M. (2014) Rhizosphere heterogeneity shapes abundance and activity of sulfur-oxidizing bacteria in vegetated salt marsh sediments. *Front Microbiol* **5**: 1–14.

Thorup, C., Schramm, A., Findlay, A.J., Finster, K.W., and Schreiber, L. (2017) Disguised as a sulfate reducer: growth of the Deltaproteobacterium Desulfurivibrio alkaliphilus by Sulfide oxidation with nitrate. *mBio* **8**: e00671-17. https://doi.org/10.1128/mBio.00671-17.

Tiedje, J.M. (1983) Denitrification: ecological niches, competition and survival. *Antonie Van Leeuwenhoek* **48**: 569-eoa.

Tiedje, J.M. (1988) Ecology of denitrification and dissimilatory nitrate reduction to ammonium. In *Biology of Anaerobic Microorganisms*. Zehnder, A.J.B. (ed.). New York, NY: John Wiley and Sons, pp. 179–244.

Tikhonova, T.V., Slutsky, A., Antipov, A.N., Boyko, K.M., Polyakov, K.M., Sorokin, D.Y., *et al*. (2006) Molecular and catalytic properties of a novel cytochrome c nitrite reductase from nitrate-reducing haloalkaliphilic sulfur-oxidizing bacterium Thioalkalivibrio nitratireducens. *Biochim Biophys Acta - Proteins Proteomics* **1764**: 715–723.

Tobias, C., and Neubauer, S.C. (2009) Salt marsh biogeochemistry - an overview. In *Coastal Wetlands: An Integrated Ecosystem Approach*, GME, P., Wolanski, E., Cahoon, D.R., and Brinson, M.M. (eds). Amsterdam, Netherlands: Elsevier, p. 445–492.

Trojan, D., Schreiber, L., Bjerg, J.T., Bøggild, A., Yang, T., Kjeldsen, K.U., and Schramm, A. (2016) A taxonomic framework for cable bacteria and proposal of the candidate genera Electrothrix and Electronema. *Syst Appl Microbiol* **39**: 297–306.

Umezawa, K., Watanabe, T., Miura, A., Kojima, H., and Fukui, M. (2016) The complete genome sequences of sulfur-oxidizing Gammaproteobacteria Sulfurifustis variabilis skN76 T and Sulfuricaulis limicola HA5 T. *Stand Genomic Sci* **11**: 1–8.

Watanabe, T., Kojima, H., Umezawa, K., Hori, C., Takasuka, T.E., Kato, Y., and Fukui, M. (2019) Genomes of neutrophilic sulfur-oxidizing chemolithoautotrophs



14622920, 2020, 6, Downloaded from https://ami-journals.onlinelibrary.wiley.com/doi/10.1111/1462-2920.14969 by <Shibboleth>-member@library.princeton.edu, Wiley Online Library on [30/01/2024]. See the Terms and Conditions (https://onlinelibrary.wiley.com/terms-and-conditions) on Wiley Online Library for rules of use; OA articles are governed by the applicable Creative Commons License

representing 9 proteobacterial species from 8 genera. *Front Microbiol* **10**: 1–13.

Weston, N. (2019) Water-column conductivity, salinity, dissolved oxygen, turbidity, and pH by deployed sonde during tidal creek lateral exchange measurements approximately every 5 minutes from beginning of flood tide to the following low tide, Rowley, MA, PIE LTER. Environmental Data Initiative. URL http://dx.doi.org/10.6073/-pasta/be36e690862648ac2efd65575d4b65b6.

Weston, N.B., Dixon, R.E., and Joye, S.B. (2006) Ramifications of increased salinity in tidal freshwater sediments: geochemistry and microbial pathways of organic matter mineralization. *J Geophys Res Biogeosci* **111**: 1–14.

Yin, G., Hou, L., Liu, M., Liu, Z., and Gardner, W.S. (2014) A novel membrane inlet mass spectrometer method to measure $^{15}NH4_4^+$ for isotope-enrichment experiments in aquatic ecosystems. *Environ Sci Technol* **48**: 9555–9562.

Yoon, S., Cruz-García, C., Sanford, R., Ritalahti, K.M., and Löffler, F.E. (2015) Denitrification versus respiratory ammonification: environmental controls of two competing dissimilatory NO3-/NO2-reduction pathways in Shewanella loihica strain PV-4. *ISME J* **9**: 1093–1104.

Zhou, Z., Takaya, N., Nakamura, A., Yamaguchi, M., Takeo, K., and Shoun, H. (2002) Ammonia fermentation, a novel anoxic metabolism of nitrate by fungi. *J Biol Chem* **277**: 1892–1896.

Zopfi, J., Kjaer, T., Nielsen, L.P., and Jorgensen, B.B. (2001) Ecology of Thioploca spp.: nitrate and sulfur storage in relation to chemical microgradients and influence of Thioploca spp. on the sedimentary nitrogen cycle. *Appl Environ Microbiol* **67**: 5530–5537.

## Supporting Information

Additional Supporting Information may be found in the online version of this article at the publisher's web-site:

**Appendix S1**. Supporting Information



14622920, 2020, 6, Downloaded from https://ami-journals.onlinelibrary.wiley.com/doi/10.1111/1462-2920.14969 by <Shibboleth>-member@library.princeton.edu, Wiley Online Library on [30/01/2024]. See the Terms and Conditions (https://onlinelibrary.wiley.com/terms-and-conditions) on Wiley Online Library for rules of use; OA articles are governed by the applicable Creative Commons License